doi:10.3788/gzxb20154402.0206001

基于相位/强度调制的伪毫米波超宽带信号的光学辅助探测

尹霄丽[1,2],韩晶晶[1],徐灿[1],郝季[1],忻向军[1],余重秀[2]
(1 北京邮电大学 电子工程学院,北京 100876)
(2 北京邮电大学 信息光子与光通信国家重点实验室,北京 100876)

摘 要:针对伪毫米波超宽带信号脉冲宽度窄且信号强度低而不易探测的特点,本文提出了两种光学辅助包络探测方案.将伪毫米波超宽带信号调制到光载波上,利用光纤布喇格光栅带通滤波器滤出调制器输出的第一边带信号,通过光电探测器和低通滤波器便可以得到用于判决的伪毫米波超宽带信号的包络信息.数学推导和仿真分析了分别采用相位调制器和强度调制器对输出包络信号振幅的影响.研究结果表明:强度调制器需要偏置控制电路来稳定偏置点的位置,当强度调制器工作在最小传输点时,得到的包络信号幅值最大;相位调制器无需偏置控制电路,其输出信号包络的幅值等于使用强度调制器的系统可得到的最大值;使用相位调制器的系统较使用强制调制器的系统具有结构更简单和插入损耗更低的特点.

关键词:相位调制;强度调制;光学辅助包络探测;伪毫米波超宽带;相位调制器;强度调制器
中图分类号:TN929.11; TN29 **文献标识码**:A **文章编号**:1004-4213(2015)02-0206001-6

Optics Assisted Envelope Detection of PMM-UWB Employing Phase/Intensity Modulation

YIN Xiao-li[1,2], HAN Jing-jing[1], XU Can[1], HAO Ji[1], XIN Xiang-jun[1], YU Chong-xiu[2]
(1 *School of Electronic Engineering, Beijing University of Posts and Telecommunications, Beijing* 100876, *China*)
(2 *State Key Laboratory of Information Photonics and Optical Communications, Beijing University of Posts and Telecommunications, Beijing* 100876, *China*)

Abstract: Pseudo millimeter wave ultra wide band signals have the characteristics of narrow pulse width, low signal strength , which make it is not easy to detect. To deal with such problem, two optics assisted envelope detection schemes were proposed. Firstly, a fiber Bragg grating was used for filtering one of the first sidebands at the output of the modulator, then the envelope of PMM-UWB signals for decision were obtained after photo-detection and low pass filter. Based on the method of mathematical derivation and numerical simulation, the effects of phase modulator or intensity modulator on the output envelope signal amplitude were analysed respectively. The results show that intensity modulator requires bias control to maintain a stable optical operating point, when the bias point of intensity modulator was switched to minimum transmission point, the maximum amplitude of envelope signals were acquired; phase modulator do not include the bias control, the amplitude of envelope in phase modulator is equal to the maximum amplitude in intensity modulator approximately. Compared with intensity modulation scheme, the phase

Foundation item: The National High Technology Research and Development Program of China (Nos. 2013AA013303, 2013AA013301, 2013AA013403)
First author: YIN Xiao-li (1970—), female, associate professor, Ph. D. degree, mainly focuses on optical information processing, optical code division multiple access, and microwave photonics. Email:yinxli@bupt.edu.cn
Contact author: HAN Jing-jing(1988—), male, M. S. degree condidate, mainly focuses on optical information processing and microwave photonics. Email:hanct@163.com
Received: Sep. 15, 2014; **Accepted**: Oct. 28, 2014

modulation scheme has more advantages, such as simple structure, low insertion loss.

Key words: Phase modulation; Intensity modulation; Optics assisted envelope detection; PMM-UWB; Phase modulator; Intensity modulator

OCIS Codes: 060.4080; 060.5060; 250.0040; 250.4110; 040.1880

0 Introduction

The Pseudo Millimeter Wave Vltra Wide Band (PMM-UWB) signals have the advantages of low power dissipation, high spatial resolution and strong anti-interference ability[1-2]. The 24 GHz-band Impulse Radio Ultra-Wideband (IR-UWB) is a special PMM-UWB signal, it can be utilized in automotive security systems, vehicular communications and short-distance high-speed wireless communications[3-4]. The 24 GHz-band IR-UWB signals should comply with the Federal Communications Commission (FCC) rules[5], its spectral density is regulated to be less than −41.3 dBm/MHz. Because of IR-UWB signals have the characteristics of narrow pulse width and low signal strength, it is very difficult to be sampled at the correct time. The novel scheme for the detection of IR-UWB signals has attracted great attention.

Recently, various IR-UWB signals detection schemes have been investigated in electric domain[6-10]. There are two main detection techniques for IR-UWB receivers, coherent and non-coherent detection. The former has some drawbacks, such as high complexity and the requirement of precise timing synchronization[6-7]. A non-coherent solution based on weighted energy detection technique of IR-UWB signal could avoid the need for incoming pulse shape estimation and complex synchronization blocks[8-10], but these techniques require either a large number of integrators or high sampling rates to estimate weighting coefficients, it will increase the complexity of the system.

Compared with electric detection techniques, optics assisted detection techniques of 24 GHz-band IR-UWB signals have been researched due to its inherent advantages such as large bandwidth, light weight, small size, and immunity to electromagnetic interference[11-12]. Both techniques employing a Mach-Zehnder electro-optical Modulator (MZM) and a Photo-Detector (PD). The MZM biased in nonlinear regime is driven by the 24 GHz-band UWB signal and the optimal coherent detection is performed by adjusting the phase of Local Oscillator (LO), however this scheme requires LO, resulting in high system complexity[11]. The MZM biased to work as conventional double sidebands (DSB) modulator and a photo-detector with low pass filter is used to carry out envelope detection, but MZM doesn't work at optimal dc bias point[12].

In the previous study[13], we have proposed a novel scheme to generate 24GHz-band IR-UWB signals using optical pulse shapers. In order to receive some 24 GHz band IR-UWB signals like generated in the paper[13-14], two optics assisted envelope detection schemes using phase modulator or Dual-Drive Mach-Zhender Modulator (DD-MZM) are proposed in this paper. The proposed schemes have simple structure and high stability. Additionally, this scheme can mitigate the requirement of synchronization and estimation of pulse shape.

1 Architecture description and mathematical model

The system scheme based on optics assisted envelope detection technique is demonstrated in Fig. 1. The 24 GHz-band IR-UWB signals can be modulated by either phase modulator or MZM into optical domain. A FBG with a circulator is connected to the modulator to filter one of the first-order sidebands, which generates optical envelope signal. Then this optical envelope signal is fed into a PD, resulting to envelope signal in electric domain. Finally a Low Pass Filter (LPF) is used to remove the high-frequency components and optimize the baseband signal.

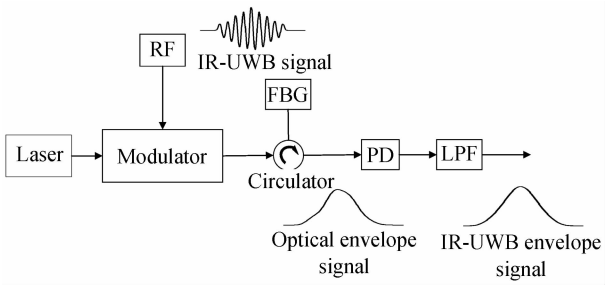

Fig. 1 Optics assisted envelope detection scheme of IR-UWB signals

1.1 Intensity modulation scheme

Fig. 2 (a) displays the intensity modulation scheme. A narrowband continuous wave of laser diode expressed as $E_{in}(t)=A_c\exp(j\omega_c t)$ is modulated by a $LiNbO_3$ DD-MZM, where A_c and ω_c are the amplitude and angular frequency, respectively.

In a push-pull MZM, the two arms signals can be written as

$$\begin{cases} V_1(t)=V_{dc1}+V_{rf}(t) \\ V_2(t)=V_{dc2}-V_{rf}(t) \end{cases} \tag{1}$$

where V_{dc1} and V_{dc2} are the dc terms, $V_{rf}(t)$ is a bandpass signal, which can be roughly modeled as[13]

$$V_{\mathrm{rf}}(t)=A_{\mathrm{m}}s_{\mathrm{B}}(t)\cos(\omega_{\mathrm{m}}t) \tag{2}$$

where A_{m} is the amplitude, $s_{\mathrm{B}}(t)$ is the equivalent baseband signal and ω_{m} is the center frequency of the IR-UWB signal.

Assuming ideal 50/50 coupling at the input and output of the MZM, the MZM output in the electric field is expressed as[15]

$$E_{\mathrm{IM}}(t)=\frac{\alpha_{\mathrm{MZM}}}{2}A_{\mathrm{c}}\exp(\mathrm{j}\omega_{\mathrm{c}}t)\times\left[\exp\left(\mathrm{j}\frac{\pi V_{\mathrm{dc1}}}{V_{\pi,\mathrm{dc}}}+\mathrm{j}\frac{\pi V_{\mathrm{rf}}(t)}{V_{\pi,\mathrm{rf}}}\right)+\exp\left(\mathrm{j}\frac{\pi V_{\mathrm{dc2}}}{V_{\pi,\mathrm{dc}}}-\mathrm{j}\frac{\pi V_{\mathrm{rf}}(t)}{V_{\pi,\mathrm{rf}}}\right)\right] \tag{3}$$

where α_{MZM} is the MZM optical loss, $V_{\pi,\mathrm{dc}}$ and $V_{\pi,\mathrm{rf}}$ are the switching bias voltage and half-wave voltage of MZM, respectively. To simplify the Eq. (3), let $V_{\mathrm{dc1}}=0$, the relative bias voltage between the two arms is $V_{\mathrm{dc}}=|V_{\mathrm{dc2}}-V_{\mathrm{dc1}}|=|V_{\mathrm{dc2}}|$. We assume that $V_{\pi,\mathrm{dc}}=V_{\pi,\mathrm{rf}}=V_{\pi}$, $E_{\mathrm{IM}}(t)$ can be expressed as

$$\begin{aligned}E_{\mathrm{IM}}(t)&=\frac{\alpha_{\mathrm{MZM}}}{2}A_{\mathrm{c}}\exp(\mathrm{j}\omega_{\mathrm{c}}t)[\exp(\mathrm{j}\phi_{\mathrm{IM}}s_{\mathrm{B}}(t)\cdot\\&\cos(\omega_{\mathrm{m}}t))+\exp(\mathrm{j}\phi_{\mathrm{dc}}-\mathrm{j}\phi_{\mathrm{IM}}s_{\mathrm{B}}(t)\cos(\omega_{\mathrm{m}}t))]=\\&\alpha_{\mathrm{MZM}}A_{\mathrm{c}}\cos\left[\frac{\phi_{\mathrm{dc}}}{2}+\phi_{\mathrm{IM}}s_{\mathrm{B}}(t)\cos(\omega_{\mathrm{m}}t)\right]\cdot\\&\exp\left[\mathrm{j}\left(\omega_{\mathrm{c}}t+\frac{\phi_{\mathrm{dc}}}{2}\right)\right]\end{aligned} \tag{4}$$

where

$$\phi_{\mathrm{dc}}=\frac{\pi V_{\mathrm{dc}}}{V_{\pi}}$$

$$\phi_{\mathrm{IM}}=\frac{\pi A_{\mathrm{m}}}{V_{\pi}}$$

Take Bessel series expansion, the Eq. (4) can be written as[16]

$$\begin{aligned}E_{\mathrm{IM}}(t)&=\alpha_{\mathrm{MZM}}A_{\mathrm{c}}\exp\left(\mathrm{j}\omega_{\mathrm{c}}t+\mathrm{j}\frac{\phi_{\mathrm{dc}}}{2}\right)\times\left\{\cos\left(\frac{\phi_{\mathrm{dc}}}{2}\right)\cdot\right.\\&\mathrm{J}_0(\phi_{\mathrm{IM}})s_{\mathrm{B}}(t)+2\sum_{n=1}^{\infty}(-1)^n\cos\left(\frac{\phi_{\mathrm{dc}}}{2}\right)\mathrm{J}_{2n}(\phi_{\mathrm{IM}})\cdot\\&s_{\mathrm{B}}(t)\cos(2n\omega_{\mathrm{m}}t)-2\sum_{n=0}^{\infty}(-1)^n\sin\left(\frac{\phi_{\mathrm{dc}}}{2}\right)\cdot\\&\left.\mathrm{J}_{2n+1}(\phi_{\mathrm{IM}})s_{\mathrm{B}}(t)\cos[(2n+1)\omega_{\mathrm{m}}t]\right\}\end{aligned} \tag{5}$$

where $\mathrm{J}_n(\ )$ is the first kind of Bessel function of order n.

For $n=0$, the two first-order sidebands of Eq. (5) can be written as

$$\begin{aligned}E_{\mathrm{IM\_F1}}(t)&=-2\alpha_{\mathrm{MZM}}A_{\mathrm{c}}\sin\left(\frac{\phi_{\mathrm{dc}}}{2}\right)\mathrm{J}_1(\phi_{\mathrm{IM}})s_{\mathrm{B}}(t)\cdot\\&\cos(\omega_{\mathrm{m}}t)\exp\left(\mathrm{j}\omega_{\mathrm{c}}t+\mathrm{j}\frac{\phi_{\mathrm{dc}}}{2}\right)=-\alpha_{\mathrm{MZM}}A_{\mathrm{c}}\sin\left(\frac{\phi_{\mathrm{dc}}}{2}\right)\cdot\\&\mathrm{J}_1(\phi_{\mathrm{IM}})s_{\mathrm{B}}(t)\exp\left(\mathrm{j}\omega_{\mathrm{c}}t+\mathrm{j}\omega_{\mathrm{m}}t+\mathrm{j}\frac{\phi_{\mathrm{dc}}}{2}\right)-\alpha_{\mathrm{MZM}}A_{\mathrm{c}}\cdot\\&\sin\left(\frac{\phi_{\mathrm{dc}}}{2}\right)\mathrm{J}_1(\phi_{\mathrm{IM}})s_{\mathrm{B}}(t)\exp\left(\mathrm{j}\omega_{\mathrm{c}}t-\mathrm{j}\omega_{\mathrm{m}}t+\mathrm{j}\frac{\phi_{\mathrm{dc}}}{2}\right)\end{aligned} \tag{6}$$

Then an FBG with a circulator is used after the MZM to filter the upper term of the two first-order sidebands, the FBG output in the electric field is

$$\begin{aligned}E_{\mathrm{IM\_F2}}(t)&=-\alpha_{\mathrm{MZM}}A_{\mathrm{c}}\sin\left(\frac{\phi_{\mathrm{dc}}}{2}\right)\mathrm{J}_1(\phi_{\mathrm{IM}})s_{\mathrm{B}}(t)\times\\&\exp\left(\mathrm{j}\omega_{\mathrm{c}}t+\mathrm{j}\omega_{\mathrm{m}}t+\mathrm{j}\frac{\phi_{\mathrm{dc}}}{2}\right)\end{aligned} \tag{7}$$

When this optical signal is sent to a Photo-Detector (PD) for square-law detection, the output current is

$$\begin{aligned}I_1(t)&=\mathscr{R}E_{\mathrm{IM\_F2}}(t)E^{*}_{\mathrm{IM\_F2}}(t)=\\&\mathscr{R}\alpha^2_{\mathrm{MZM}}A_{\mathrm{c}}^2\sin^2\left(\frac{\phi_{\mathrm{dc}}}{2}\right)\mathrm{J}_1^2(\phi_{\mathrm{IM}})s_{\mathrm{B}}^2(t)\end{aligned} \tag{8}$$

where $\mathscr{R}$ is the responsivity of PD.

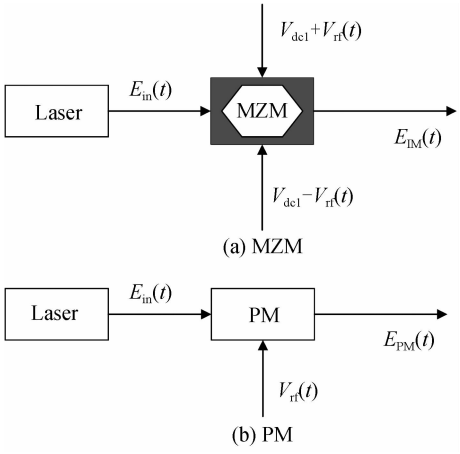

Fig. 2 Modulation scheme employing

The intensity transmission response of MZM has the form of raised cosine function. From Eq. (8) we can see, that the envelope of IR-UWB $s_{\mathrm{B}}^2(t)$ can be detected, which amplitude is determined by ϕ_{dc}, which is determined by the relative dc bias voltage V_{dc}.

It can be seen from Fig. 3, that we need to set the

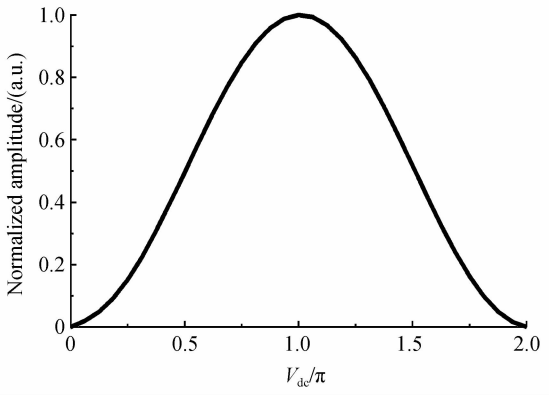

Fig. 3 The normalized intensity of the envelope of IR-UWB as a function of V_{dc}

appropriate dc bias point to take advantage of different modulation region. If we switch the bias point of MZM to quadrature point, that is to say, the relative dc voltage becomes $V_{\pi}/2$, the modulation scheme can be described as DSB scheme. If we switch the bias point of MZM to minimum transmission point, that is to say, relative dc voltage becomes V_{π}, the modulation scheme can be described as Optical Carrier Suppression (OCS) scheme, in this way the half-wave rectification is achieved and the maximum amplitude is acquired. The

output current of PD is

$$I_1(t)=\begin{cases}\dfrac{\mathscr{R}\alpha_{\mathrm{MZM}}^2A_{\mathrm{c}}^2}{2}\mathrm{J}_1^2(\phi_{\mathrm{IM}})s_{\mathrm{B}}^2(t) & \text{DSB scheme}\\ \mathscr{R}\alpha_{\mathrm{MZM}}^2A_{\mathrm{c}}^2\mathrm{J}_1^2(\phi_{\mathrm{IM}})s_{\mathrm{B}}^2(t) & \text{OCS scheme}\end{cases} \tag{9}$$

1.2 Phase modulation scheme

Fig. 2 (b) depicts the phase modulation scheme with $LiNbO_3$ phase modulator, which has only one arm without dc term.

The output of phase modulator can be expressed as

$$E_{\mathrm{PM}}(t)=\alpha_{\mathrm{PM}}A_{\mathrm{c}}\exp(\mathrm{j}\omega_{\mathrm{c}}t)\exp\left[\mathrm{j}\frac{\pi}{V_{\pi,\mathrm{PM}}}V_{\mathrm{rf}}(t)\right]=$$
$$\alpha_{\mathrm{PM}}A_{\mathrm{c}}\exp(\mathrm{j}\omega_{\mathrm{c}}t)\exp\left[\mathrm{j}\frac{\pi}{V_{\pi,\mathrm{PM}}}A_{\mathrm{m}}s_{\mathrm{B}}(t)\cos(\omega_{\mathrm{m}}t)\right] \tag{10}$$

where $V_{\pi,\mathrm{PM}}$ is the half-wave voltage of phase modulator and α_{PM} is the PM optical loss.

Take Bessel series expansion, the Eq. (10) can be written as[16]

$$E_{\mathrm{PM}}(t)=\alpha_{\mathrm{PM}}A_{\mathrm{c}}\exp(\mathrm{j}\omega_{\mathrm{c}}t)\{\mathrm{J}_0(\phi_{\mathrm{PM}})s_{\mathrm{B}}(t)+2\sum_{n=1}^{\infty}(-1)^n\cdot$$
$$\mathrm{J}_{2n}(\phi_{\mathrm{PM}})s_{\mathrm{B}}(t)\cos(2n\omega_{\mathrm{m}}t)+2\mathrm{j}\sum_{n=0}^{\infty}(-1)^n$$
$$\mathrm{J}_{2n+1}(\phi_{\mathrm{PM}})s_{\mathrm{B}}(t)\cos[(2n+1)\omega_{\mathrm{m}}t]\} \tag{11}$$

where

$$\phi_{\mathrm{PM}}=\frac{\pi A_{\mathrm{m}}}{V_{\pi,\mathrm{PM}}}$$

For $n=0$, the two first-order sidebands of Eq. (11) can be written as

$$E_{\mathrm{PM\_F1}}(t)=2\mathrm{j}\alpha_{\mathrm{PM}}A_{\mathrm{c}}\mathrm{J}_1(\phi_{\mathrm{PM}})s_{\mathrm{B}}(t)\cos(\omega_{\mathrm{m}}t)\cdot$$
$$\exp(\mathrm{j}\omega_{\mathrm{c}}t)=\mathrm{j}\alpha_{\mathrm{PM}}A_{\mathrm{c}}\mathrm{J}_1(\phi_{\mathrm{PM}})s_{\mathrm{B}}(t)\cdot$$
$$\exp(\mathrm{j}\omega_{\mathrm{c}}t+\mathrm{j}\omega_{\mathrm{m}}t)+\mathrm{j}\alpha_{\mathrm{PM}}A_{\mathrm{c}}\mathrm{J}_1(\phi_{\mathrm{PM}})s_{\mathrm{B}}(t)\cdot$$
$$\exp(\mathrm{j}\omega_{\mathrm{c}}t-\mathrm{j}\omega_{\mathrm{m}}t) \tag{12}$$

Then an FBG with a circulator is used after the phase modulator to filter the upper term of the two first-order sidebands. The FBG output in the electric field is

$$E_{\mathrm{PM\_F2}}(t)=\mathrm{j}\alpha_{\mathrm{PM}}A_{\mathrm{c}}\mathrm{J}_1(\phi_{\mathrm{PM}})s_{\mathrm{B}}(t)\exp(\mathrm{j}\omega_{\mathrm{c}}t+\mathrm{j}\omega_{\mathrm{m}}t) \tag{13}$$

When this optical signal is sent to a PD for square-law detection, the output current is

$$I_2(t)=\mathscr{R}E_{\mathrm{PM\_F2}}(t)E_{\mathrm{PM\_F2}}^{*}(t)=$$
$$\mathscr{R}\alpha_{\mathrm{PM}}^2A_{\mathrm{c}}^2\mathrm{J}_1^2(\phi_{\mathrm{PM}})s_{\mathrm{B}}^2(t) \tag{14}$$

where $\mathscr{R}$ is the responsivity of PD.

2 Simulation and discussion

Numerical simulation is performed to compare and verify the two different modulation schemes. The 24 GHz-band IR-UWB signal waveform and spectrum are given in Fig. 4. This signal has the characteristics of narrow pulse width and low amplitude.

In the simulation we set the optical loss of modulator as $\alpha_{\mathrm{MZM}}=\alpha_{\mathrm{PM}}=1$ and the amplitude of 24 GHz band IR-UWB signal as $A_{\mathrm{m}}=1$ mV. The phase modulator and MZM have the same half-wave voltage $V_{\pi}=V_{\pi,\mathrm{PM}}=4$ V.

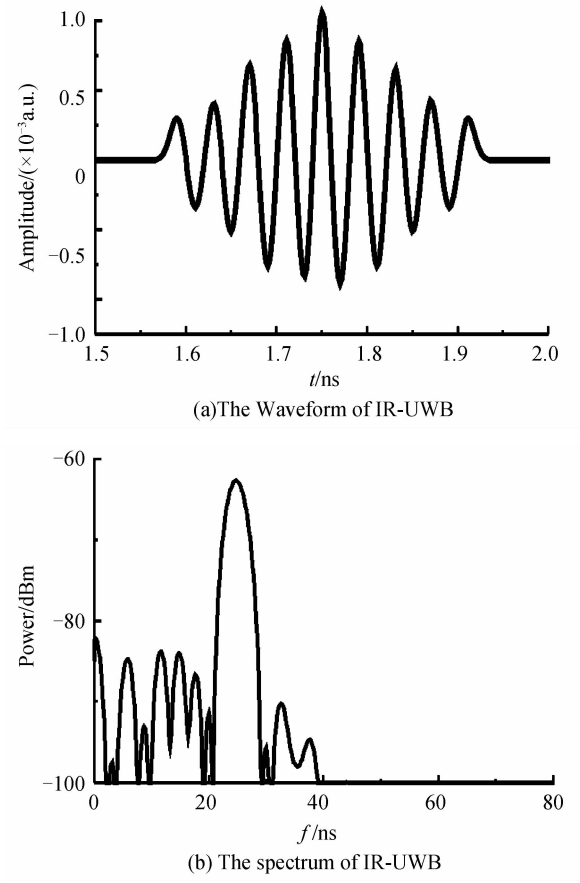

Fig. 4 Waveform and spectrum of 24 GHz band IR-UWB signal and spectrum

In intensity modulation scheme, the system works at DSB modulation type for $V_{\mathrm{dc}}=2$ V and OCS modulation type for $V_{\mathrm{dc}}=4$ V, respectively. An FBG, which −3 dB filter bandwidth is 25 GHz, with a circulator is used after the modulator to filter the upper term of the two first-order sidebands. Then this optical signal is sent to a PD for square-law detection, resulting to envelope signal of IR-UWB in electric domain.

Fig. 5 shows the simulation results for the output signal and spectrum of modulator as well as the spectrum of FBG. By using two different kind of modulators and changing the relative dc voltageV_{dc}, the output signal and spectrum of modulators are shown in Fig. 5 (a)～(f), and the output spectrum of FBG in three different schemes is depicted in Fig. 5 (g)～(i). Comparing the three output spectrum of FBG, we can clearly observe that the first sideband spectrum of PM scheme is approximate to OCS scheme, and the first sideband spectrum of DSB scheme has more 3 dB optical power loss.

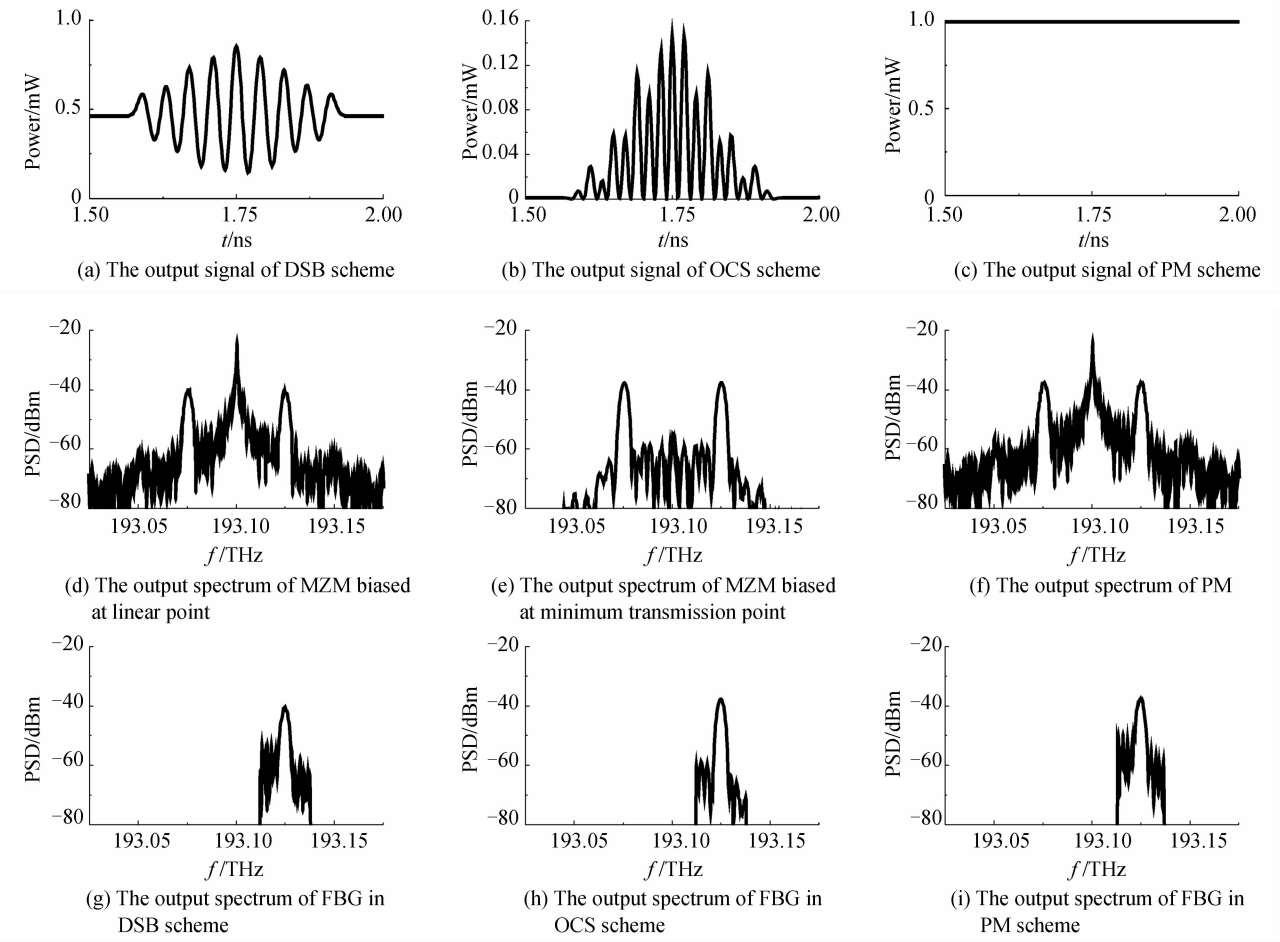

Fig. 5 The simulation results for the output signal and spectrum of modulator as well as the spectrum of FBG using the proposed scheme

Fig. 6 show the envelopes of IR-UWB signal using different kind of modulation scheme, such as OCS scheme, DSB scheme and PM scheme. As we can see from Fig. 6 that the amplitude of envelope in PM scheme is equal to that one in OCS scheme approximately, both are two times as that one in DSB scheme.

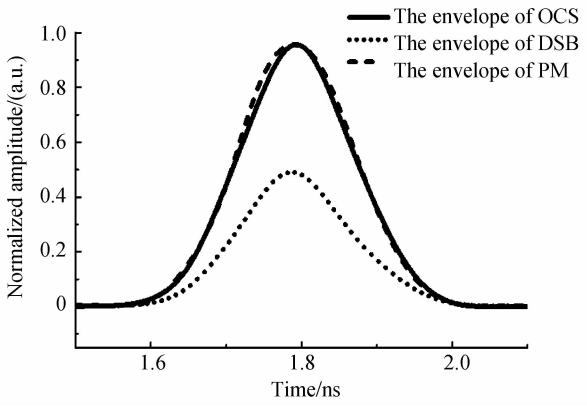

Fig. 6 The envelopes of IR-UWB signal using intensity modulation or phase modulation

Fig. 7 and Fig. 8 show the electric signal eye diagrams of PM scheme and OCS scheme, respectively. The amount of distortion of OCS scheme

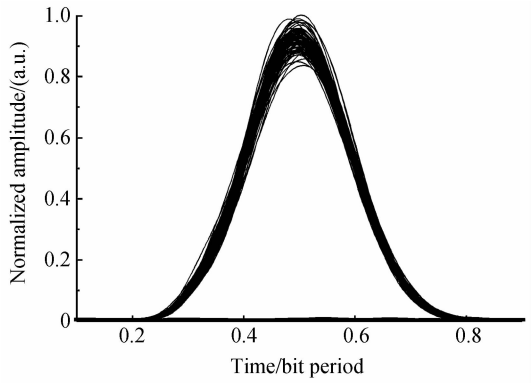

Fig. 7 Electric signal eye diagrams of PM scheme output

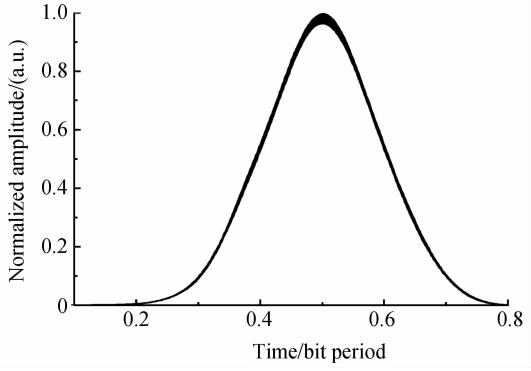

Fig. 8 Electric signal eye diagram of OCS scheme output

is less than PM scheme slightly, which can be explained that there is no frequency chirp phenomenon in a push-pull MZM.

However, from the perspective of system structure complexity, the PM scheme is better than IM scheme. In intensity modulation scheme, the MZM not only requires bias control to maintain a stable optical operating point but also includes the relative time delay control to generate the pull-push signal. The advantages of PM scheme are the elimination of the bias control, simple structure and low insertion loss.

3 Conclusion

In this paper, we demonstrate two optics assisted envelope detection schemes of PMM-UWB signals employing phase modulation or intensity modulation. The detailed mathematical derivation and numerical simulation show that the maximum amplitude of the detected envelope can be obtained via OCS modulation in the IM scheme and the amplitude of envelope in PM scheme is equal to the one in OCS scheme approximately. Compared with the IM scheme, the PM scheme has more advantages, such as simple structure, low insertion loss and elimination of the bias control.

References

[1] PORCINO D, HIRT W. Ultra-wideband radio technology: potential and challenges ahead [J]. *IEEE Communications Magazine*, 2003, **41**(7): 66-74.

[2] STROHM K M, BLOECHER H L, SCHNEIDER R, *et al*. Development of future short range radar technology [C]. Proceedings of European Radar Conference, 2005, 165-168.

[3] AIELLO G R, ROGERSON G D. Ultra-wideband wireless systems [J]. *IEEE Microwave Magazine*, 2003, **4**(2): 36-47.

[4] DOMINIK H. Short range radar-status of UWB sensors and their applications [C]. Proceedings of European Radar Conference, 2007, 251-254.

[5] The US FCC regulation on 24 GHz UWB SRR Code of federal regulations [s]. In: Title 47, Chapter 1, Part 15, Subpart F, no. 15. 515.

[6] DAWOOD M, NARAYANAN R M. Receiver operating characteristics for the coherent UWB random noise radar [J]. *IEEE Transactions on Aerospace and Electronic Systems*, 2001, **37**(2): 586-594.

[7] WANG X, YOUNG A, PHILIPS K, *et al*. Clock accuracy analysis for a coherent IR-UWB system [C]. Proceedings of IEEE Ultra-Wideband International Conference, 2011, 440-444.

[8] D'AMICO A A, MENGALI U. Energy-Detection UWB Receivers with Multiple Energy Measurements [J]. *IEEE Transactions on Wireless Communications*, 2007, **6**(7): 2652-2659.

[9] WANG F, TIAN Z, SADLER B M. Weighted energy detection for noncoherent ultra-wideband receiver design [J]. *IEEE Transactions on Wireless Communications*, 2011, **10**(2): 710-720.

[10] JI S A, LEE S J, KIM J S. Simplified structure of weighted energy detector for UWB-IR systems [J]. *Electronics Letters*, 2012, **48**(1): 48-50.

[11] GUENNEC Y L, GARY R. Optical frequency conversion for millimeter-wave ultra-wideband-over-fiber systems [J]. *IEEE Photonics Technology Letters*, 2007, **19**(13): 996-998.

[12] KURI T, OMIYA Y, KAWANISHI T, *et al*. Optical transmitter and receiver of 24-GHz ultra-wideband signal by direct photonic conversion techniques [C]. Proceedings of IEEE International Topical Meeting on Microwave Photonics, 2006, 1-4.

[13] YIN X, TU J, CHEN Y, *et al*. Optimization of 24 GHz-band impulse radio ultra-wideband optical signal generator [J]. *Optics Communications*, 2013, **287**: 85-89.

[14] NAKAMURA K, HANAWA M, NONAKA K. 24 GHz-band UWB-IR pulse generation using optical signal processing [C]. Proceedings of IEEE OptoElectronics and Communications Conference, 2009, 1-2.

[15] CARTLEDGE J C. Performance of 10 Gb/s lightwave systems based on lithium niobate Mach-Zehnder modulators with asymmetric Y-branch waveguides [J]. *Photonics Technology Letters*, 1995, **7**(9): 1090-1092.

[16] HUANG C, CHEN L, YU J, WEN S. Millimeter-wave generation utilizing one phase modulator[J]. *Chinese Journal of Lasers*, 2008, **35**(1): 73-76.